

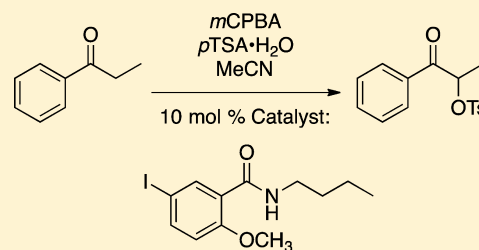
# Relative Rate Profiles of Functionalized Iodoarene Catalysts for Iodine(III) Oxidations

Timothy R. Lex, Maria I. Swasy, and Daniel C. Whitehead\*

Department of Chemistry, Clemson University, Clemson, South Carolina 29634, United States

**S** Supporting Information

**ABSTRACT:** A series of rate studies were conducted to evaluate the steric and electronic properties that govern the reactivity of iodoarene amide catalysts in the  $\alpha$ -oxytosylation of propiophenone. A meta-substituted benzamide catalyst emerged as the most reactive. This catalyst was employed in the  $\alpha$ -oxytosylation of a series of substituted propiophenones, returning the  $\alpha$ -tosyloxy ketone products in excellent isolated yield.



## INTRODUCTION

Recently, a number of hypervalent iodine reagents have been developed and utilized for a variety of synthetically useful transformations.<sup>1–3</sup> Compared to transition-metal catalysts, I(III) catalysts and reagents are advantageous due to their availability, applicability, and lower toxicity.<sup>3–5</sup> Traditionally, hypervalent iodine reagents have been used as mild and highly selective oxidants and electrophiles in various oxidation and oxygenation reactions.<sup>6,7</sup> Some of the more notable transformations include the oxidations of sulfides to sulfoxides,<sup>8</sup> the conversion of alcohols to their corresponding carbonyl compounds,<sup>9–11</sup> alkene functionalizations,<sup>12–14</sup> oxidative dearomatization of phenols,<sup>15–17</sup>  $\alpha$ -functionalization of carbonyl compounds,<sup>1,18,19</sup> and oxidative lactonizations.<sup>20–22</sup> For most of the aforementioned reactions, aryl- $\lambda^3$ -iodanes [i.e., hypervalent iodine compounds bearing two heteroatom ligands and one aryl functionality on the iodine(III) center] have been successfully employed. Well-known and commercially available  $\lambda^3$ -iodanes include (diacetoxyiodo)benzene (PIDA),<sup>23–25</sup> [bis-(trifluoroacetoxy)iodo]benzene (PIFA),<sup>26,27</sup> and hydroxy-(tosyloxy)iodobenzene (HTIB or Koser's reagent).<sup>28</sup>

Historically, the use of stoichiometric amounts of hypervalent iodine reagents has been essential for mediating the desired transformations. Conversely, organocatalysts are broadly applicable, while concomitantly avoiding the cost and toxicity issues that arise when using analogous metal-based catalysts.<sup>29–31</sup> The ability to use catalytic amounts of iodoarene reagents, by using a co-oxidant to generate the iodine(III) species in situ, has proven to be a pivotal development for the practical applicability of hypervalent iodine chemistry.<sup>8,32,33</sup> The first catalytic use of iodoarene reagents was autonomously disclosed by the groups of both Ochiai<sup>34</sup> and Kita<sup>35,36</sup> in order to perform catalytic  $\alpha$ -oxidations of ketones and catalytic oxidative spirocyclizations of phenols, respectively. Shortly following, Ishihara and co-workers reported the successful implementation of iodoarene hypervalent iodine(III) catalysts

to facilitate the lactonization of  $\gamma$ -benzoylcarboxylic acids to  $\gamma$ -benzoyl- $\gamma$ -lactones.<sup>20</sup>

Our group is interested in the investigation of hypervalent iodine(III) organocatalysts in order to promote synthetically valuable bond-forming reactions. In this disclosure, we examined the catalytic performance of a series of iodoarene amide catalysts with varying electronic and steric demands for the  $\alpha$ -oxygenation of ketones in stoichiometric and catalytic fashions. The  $\alpha$ -oxygenation reaction serves as an important synthetic transformation because it installs a new stereocenter with a synthetically useful leaving group in the  $\alpha$ -position relative to the carbonyl moiety, resulting in functionalized products with valuable synthetic applications.<sup>37</sup>

Considerable efforts to induce high yields in the  $\alpha$ -functionalization of ketones have been reported in the literature. Below are a few representative examples of the  $\alpha$ -oxygenation of ketones in stoichiometric and catalytic fashions. Using a stoichiometric amount of HTIB, Koser et al. were the first to successfully convert ketones to their corresponding  $\alpha$ -oxygenated products in good yields (40–94%).<sup>38</sup> Soon after, Moriarty et al. were able to effect the same transformation in moderate to excellent yields (78–92%) by implementing HTIB and trimethylsilyl enol ethers.<sup>39</sup> In a similar fashion, Nabana and Togo reported the use of substituted [hydroxy(tosyloxy)-iodo]arenes and noticed increased reactivity with arenes bearing trifluoromethyl substituents, specifically producing the  $\alpha$ -oxygenated propiophenone in a 96% isolated yield.<sup>40</sup> Ochiai reported the  $\alpha$ -acetoxylation of ketones by employing both a catalytic amount of iodobenzene and *m*CPBA as a stoichiometric terminal oxidant in acetic acid to obtain the desired product in moderate isolated yields (43–63%).<sup>34</sup> Yamamoto and Togo extended this work with the use of *p*-toluenesulfonic acid in acetonitrile accompanied by a catalytic amount of iodobenzene for the generation of a variety of  $\alpha$ -oxygenated

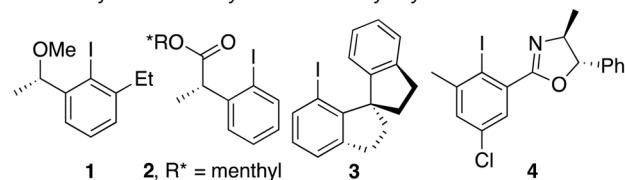
Received: September 15, 2015

Published: November 24, 2015

ketones in decent yields (63–88%).<sup>41</sup> Furthermore, Togo and co-workers successfully supplied  $\alpha$ -oxytosylacetophenone with recyclable polystyrene-supported iodoarene catalysts and noted iodobenzene to be a more effective catalyst than *p*-methyl-, *p*-methoxy-, and *p*-chloro-substituted iodoarenes.<sup>42</sup> Wirth and colleagues applied iodoxolone-based hypervalent iodine reagents and reported rate enhancements, with 22–54% conversions, when fluorinated iodoxolones were used for the  $\alpha$ -oxytosylation of ketones.<sup>43</sup> Yan and co-workers expanded the applicability of polyvalent iodine catalysts by utilizing alkyl-substituted iodide species to furnish various  $\alpha$ -sulfonyloxy ketones (27–95% yields).<sup>44</sup> More recently, Basdevant and Legault used HTIB to enable the rapid transformation of enol esters to afford  $\alpha$ -substituted ketones in excellent yields.<sup>45</sup>

Currently, there is an increased interest in rendering these types of reactions enantioselective.<sup>2,46,47</sup> Figure 1 depicts a

Known asymmetric catalysts for the  $\alpha$ -oxytosylation of ketones:



Our Approach:

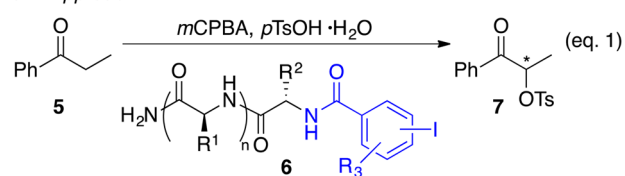


**Figure 1.** State of the art catalysts for the asymmetric hypervalent-iodine-mediated  $\alpha$ -oxytosylation of ketones. Our peptide-based approach is shown in eq 1.

series of the most selective catalysts (1–4) known for the direct enantioselective  $\alpha$ -oxytosylation of ketones, a transformation that has remained relatively recalcitrant to synthetically useful levels of enantioinduction despite a number of studies.<sup>2,19,46</sup> Wirth and colleagues developed a collection of hypervalent

iodoarene catalysts that situate the chiral moiety ortho to the iodine atom (e.g., 1 and 2).<sup>47,48</sup> Catalysts 1 and 2 effected the enantioselective  $\alpha$ -oxytosylation of propiophenone in 27 and 39% ee, respectively. Zhang and co-workers disclosed the axially chiral iodoarene 3, which returned  $\alpha$ -tosyloxypropiophenone (i.e., 7) in 53% ee.<sup>49</sup> The Legault laboratory disclosed catalyst 4, bearing an ortho-disposed chiral oxazoline moiety, which was capable of generating 7 in 48% ee.<sup>50,51</sup> While all three of these groups have made pioneering advances toward realizing a synthetically relevant catalytic enantioselective  $\alpha$ -oxytosylation reaction, the scaffolds each possess some limitations that may hinder further optimization to higher enantioselectivities. First, with the arguable exception of the Legault scaffold, they are not particularly amenable to iterative catalyst structural tuning with the aim of improving enantioselectivity. For example, catalyst 3 arises from a seven-step linear synthesis.<sup>49</sup> Second, all four catalyst scaffolds rely on positioning the chiral moiety exclusively ortho to the iodine atom in order to project the stereochemical information in proximity to the I(III) catalytic site, which may somewhat limit the ability to fully optimize the catalyst structure. For instance, positioning substituents ortho to the iodine active site can significantly retard the reactivity of the catalyst (see below for details). Very recently, the Legault group reported a breakthrough in the enantioselective  $\alpha$ -oxytosylation of related enol acetates by the action of the well-known bis-lactate-derived iodoarene catalysts, returning the desired  $\alpha$ -tosyloxy ketone products with selectivities less than or equal to 90% ee.<sup>52</sup> Nevertheless, highly enantioselective direct  $\alpha$ -oxytosylations of the parent ketone substrate are still elusive.

Our group has been pursuing a strategy to overcome these limitations via the incorporation of the catalytically active iodoarene group onto highly modular, readily accessible chiral peptides via a benzamide linkage (e.g., generic catalyst 6, Figure 1, eq 1). In this strategy, the amide bond linkage provides a simple route for the installation of the iodoarene moiety into a chiral peptide framework. Further, we hypothesized that we might overcome the requirement for ortho-disposed chirality on the iodoarene catalyst by leveraging the exceptional modularity and available rigidifying secondary structural motifs afforded by a peptide-based scaffold.<sup>53,54</sup>

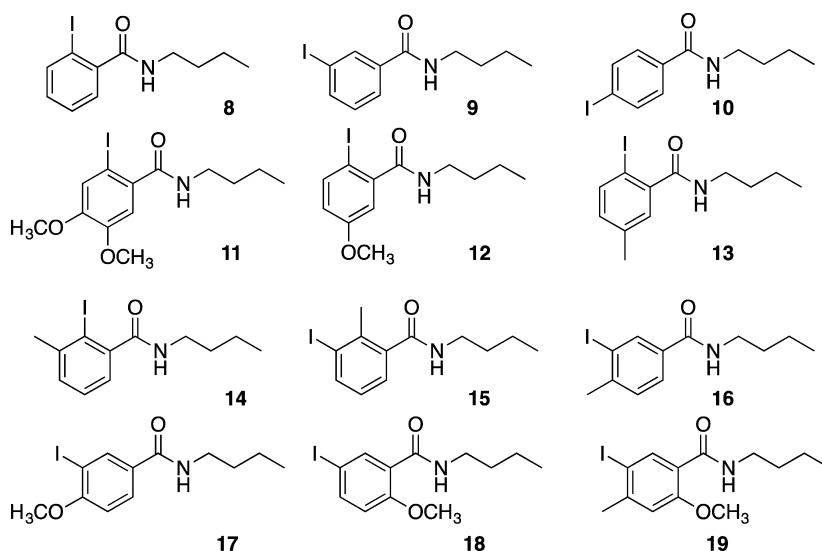


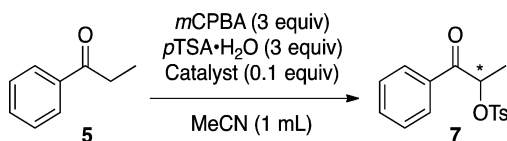
**Figure 2.** Iodoarene amide catalyst structures.

With this overall strategy in mind, we surmised that the benzamide linkage, required in our strategy to couple the iodoarene catalytic site to the peptide scaffold, might have profound effects on the reactivity of the resultant chiral peptide iodoarene catalyst, thus providing motivation for the study described herein. In order to probe the effect of the benzamide linkage on the reactivity of the iodoarene catalyst, we synthesized a series of *N*-butyl-iodobenzamide catalysts with the goal of understanding the electronic and steric influence of the benzamide substituent on the iodoarene catalyst. The details of this study are presented below.

## RESULTS AND DISCUSSION

A selection of *N*-butyl-iodobenzamides (i.e., 8–19) were prepared from the corresponding carboxylic acids by means of a conventional amidation reaction via formation of the acid chloride and displacement by *N*-butylamine (Figure 2). Our investigation began with the  $\alpha$ -oxytosylation of propiophenone, utilizing reaction conditions similar to those previously reported, namely, iodoarene derivatives (0.1 equiv) as the precatalyst with *m*-chloroperoxybenzoic acid (*m*CPBA, 3 equiv) as the co-oxidant, *p*-toluenesulfonic acid monohydrate (*p*TSA·H<sub>2</sub>O, 3 equiv) as the nucleophile, and acetonitrile (MeCN, 1 mL) as the solvent at room temperature (Scheme 1).<sup>38,41</sup> A

Scheme 1. Oxidative  $\alpha$ -Oxytosylation of Propiophenone

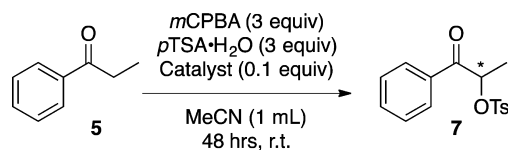


brief workup of the reaction mixture was also necessary in order to isolate the desired product for GC analysis. Reactions were quenched with dimethyl sulfide (3 equiv) at prescribed times followed by GC analysis. Yields were calculated from a product standard curve in concentrations ranging from 0.005 to 0.1 M. Reported yields and standard deviations were collected from averaged triplicate runs, with tetraglyme (0.05 M) being employed as the internal standard.

Initial investigations began with iodoenzamides 8–10 at room temperature for 48 h in order to compare the relative rates of catalysis in the  $\alpha$ -oxytosylation of propiophenone when the amide functionality was situated ortho, meta, and para relative to the iodine atom, respectively. At the prescribed 48 h time point, the reactions were quenched by the addition of 3 equiv of dimethyl sulfide to reduce the remaining *m*CPBA co-oxidant. It was clear that catalysts 9 and 10 with the amide in the meta- and para-positions on the arene were more reactive than the ortho-substituted iodoarene 8, resulting in >99%, 82%, and 3% yields, respectively (entries 1–3, Table 1). Evidently, the *o*-iodobenzamide catalyst 8 imparts a combination of steric encumbrance and inductive electron withdrawal that results in a significantly unreactive catalyst. Interestingly, the electron withdrawal due to positioning the iodine para relative to the benzamide (i.e., 10) evidently does not significantly hinder the rate of reaction.

Following these initial results, a variety of substituted iodoarene amide derivatives 11–14 were prepared to probe the influence of electronics and sterics on the rate of the sluggish *o*-iodobenzamide 8 (Figure 1). Catalysts 11–13 represent iodoarenes with the amide substituent located in

Table 1. Oxidative  $\alpha$ -Oxytosylation of Propiophenone for 48 h at Room Temperature



entry	catalyst	yield (%) <sup>a,b</sup>
1	8	3 ± 0
2	9	quant.
3	10	82 ± 6
4	11	2 ± 0
5	12	2 ± 0
6	13	3 ± 0
7	14	29 ± 4
8	15	91 ± 3
9	16	76 ± 3
10	17	67 ± 4
11	18	quant.
12	19	quant.

<sup>a</sup>Average yields of triplicate runs employing tetraglyme as the internal standard. <sup>b</sup>On 0.1 mmol scale.

the ortho position with respect to the iodine along with the incorporation of electron-donating substituents (i.e., OMe and Me) on the arene. Catalyst 11 bears two methoxy substituents, while catalysts 12 and 13 bear a para (relative to I) methoxy and methyl substituent, respectively. The groups of Wirth<sup>47</sup> and Legault<sup>50</sup> independently observed that electron-releasing substituents para relative to I imparted modest increases in reactivity with other iodoarene catalysts. Additionally, we surmised that the second methoxy group resident on catalyst 11 (i.e. meta with respect to I and para to the amide) might serve to enhance catalyst activity relative to the parent *o*-iodobenzamide 8 by attenuating the electron-withdrawing capacity of the amide moiety. Additionally, we prepared catalyst 14, representing a direct analog of the “hypervalent twist” catalysts pioneered by Su and Goddard<sup>55</sup> and expanded upon by Legault’s group.<sup>47,50</sup>

Next, catalysts 11–14 were employed in the  $\alpha$ -oxytosylation of propiophenone for 48 h (Table 1, entries 4–7). In our hands, the incorporation of electron donors in the ortho and para positions relative to the iodine atom did little to improve on the sluggish rate of reaction observed for the parent *o*-iodobenzamide 8. The incorporation of two (i.e., 11) or one methoxy group on the arene both returned product in just 2% yield over 48 h (entries 4 and 5). Similarly, positioning a methyl group para to the I (catalyst 13) returned a 3% yield after 48 h (entry 6). Interestingly, catalyst 14 exhibited a significant rate enhancement, returning the  $\alpha$ -oxytosylated ketone product in a 29% yield after 48 h. This result recapitulates the hypervalent twist phenomenon that accelerates the nucleophilic attack of the substrate enol tautomer on the I(III) reagent.<sup>50,55</sup> Nevertheless, catalyst 14 is still significantly slower than the *p*- and *m*-iodobenzamides 9 and 10 (cf. entries 2 and 3).

We hypothesize that the significant reduction in reactivity of the *o*-iodobenzamides relative to the para and meta congeners results from divergent rate enhancement phenomena. Legault and co-workers demonstrated that the I(I) to I(III) oxidation of analogs of 8 and 14 proceed at identical rates. Thus, the rate enhancement due to the hypervalent twist results from a lowering of the activation energy for the formation of the  $\alpha$ -

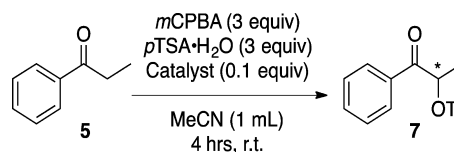
iodonium propiophenone intermediate arising from the attack of the enol tautomer of the substrate.<sup>47,50,55</sup> Stated differently, the coordination of the ortho-situated Lewis base (i.e., the amide) imparts significant stabilization of the I(III) analog of **8**, thus slowing the rate of its displacement by the enol nucleophile. In the case of catalyst **14**, incorporation of the *o*-methyl group induces a destabilizing twist in the I(III) complex, effectively lowering the activation energy of the enol displacement relative to the situation with catalyst **8**.<sup>47,50</sup> Conversely, when comparing the relative rates of catalysts **8**–**10**, we hypothesize that the lack of an appropriately positioned Lewis base in **9** and **10** precludes such stabilization of the I(III) intermediate, thus leading to significant rate acceleration relative to catalyst **8**.

Given that our original experiments revealed that the *m*-iodobenzamide catalyst **9** exhibited the fastest relative rate, we next prepared a series of substituted analogs that maintain the meta relationship between the I atom and the benzamide moiety. Thus, we prepared catalysts **15**–**19** (Figure 1). Catalysts **15** and **16** were designed to probe the effect of *o*-methyl substitution relative to I while simultaneously maintaining the position of that atom meta to the benzamide. Essentially, these two catalysts were designed to probe whether the hypervalent twist phenomenon is operable in catalysts where the Lewis base (i.e., the benzamide) is oriented meta to the iodine atom and is thus inaccessible for coordination. Catalysts **17** and **18** were designed to probe the influence of positioning an electron-donating methoxy substituent either ortho or para to the iodine atom while the benzamide was maintained in the meta position. Finally, catalyst **19** combined the incorporation of an ortho-substituted methyl and a para-situated methoxy group relative to iodine, while the meta-disposed benzamide was maintained.

Thus, we quenched the reactions promoted by these catalysts after 48 h at room temperature and subjected them to GC analysis in triplicate (Table 1, entries 8–12). Catalysts **15**–**19** all efficiently promoted the  $\alpha$ -oxytosylation of propiophenone, returning product in yields ranging from 67% to >99%. Of the group, catalysts **15** (91% yield) and **18** and **19** (each quantitative) were the most active.

In order to further probe the relative rates of the most active catalysts in our 48 h screen, we subjected the seven most active catalysts (**9**, **10**, and **15**–**19**) to a quench after just 4 h (Table 2). Iodoarene catalysts with the amide in the meta-position showed the greatest rate enhancement, while the corresponding *p*-iodobenzamide **10** performed the worst in this abbreviated series of catalysts. Catalyst **18** afforded the desired  $\alpha$ -oxytosylated product in 44% yield (entry 6, Table 2), followed by **9** with 39% yield (entry 1, Table 2). This observation led to a final structural modification to **18** with the introduction of a methyl group ortho to the iodine in hopes to generate a more reactive catalyst **19** via the hypervalent twist described by Su and Goddard<sup>55</sup> and Guilbault and Legault.<sup>50</sup> Recall from the 48-h screen (Table 1) that catalyst **14** showed a moderate rate enhancement, resulting in a 29% yield compared to catalyst **8** with a 3% yield of the  $\alpha$ -oxytosylated product, which is in accordance with the hypervalent twist concept (Table 1, entries 7 and 1). In contrast to the hypervalent twist model with ortho-situated Lewis bases, **19** showed no further rate enhancement, producing the  $\alpha$ -oxytosylated product in a modest 40% yield (entry 7, Table 2). Likewise, rate reductions were observed with catalysts **15** and **16**, which possess steric bulk in the ortho position (with respect to the iodine), relative to catalyst **9**,

**Table 2. Oxidative  $\alpha$ -Oxytosylation of Propiophenone for 4 h at Room Temperature**



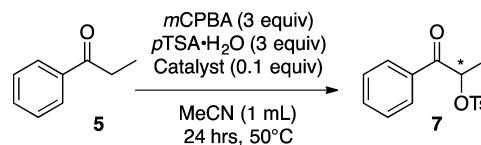
entry	catalyst	yield (%) <sup>a,b</sup>
1	9	39 ± 3
2	10	19 ± 3
3	15	28 ± 2
4	16	24 ± 3
5	17	36 ± 1
6	18	44 ± 2
7	19	40 ± 1

<sup>a</sup>Average yields of triplicate runs employing tetraglyme as the internal standard. <sup>b</sup>On 0.1 mmol scale.

which bears no steric influence (Table 2, entries 3, 4, and 1). Taken together, these data further underscore that the rate acceleration observed due to the hypervalent twist phenomenon is only operative in aryl iodides substituted with ortho-oriented Lewis bases. Further, comparing the relative rates of the reaction catalyzed by the unmodified *m*-iodobenzamide **9** with more electron-rich substituted derivatives **17**–**19** highlights that electronic effects on the iodoarene may play a relatively minor role in the rate of catalysis for the  $\alpha$ -oxytosylation reaction.

Next, all 12 iodoarene amides were screened at 50 °C for 24 h (Table 3). In this study, the trends observed for the room-

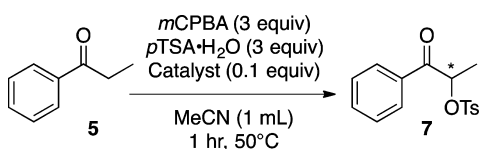
**Table 3. Oxidative  $\alpha$ -Oxytosylation of Propiophenone for 24 h at 50 °C**



entry	catalyst	yield (%) <sup>a,b</sup>
1	8	16 ± 4
2	9	96 ± 2
3	10	96 ± 3
4	11	11 ± 3
5	12	12 ± 2
6	13	16 ± 3
7	14	65 ± 1
8	15	92 ± 4
9	16	quant.
10	17	quant.
11	18	97 ± 2
12	19	60 ± 5

<sup>a</sup>Average yields of triplicate runs employing tetraglyme as the internal standard. <sup>b</sup>On 0.1 mmol scale.

temperature reactions were recapitulated at 50 °C. Catalysts **9**, **10**, and **15**–**19** all resulted in moderate to excellent yields and accordingly were rescreened at 50 °C for 1 h (Table 4). Similar to the room-temperature screens, catalyst **18** proved to be the most reactive, affording the  $\alpha$ -oxytosylated propiophenone in a 68% yield, followed by **9** and **17** (entries 6, 1, and 5, Table 4).

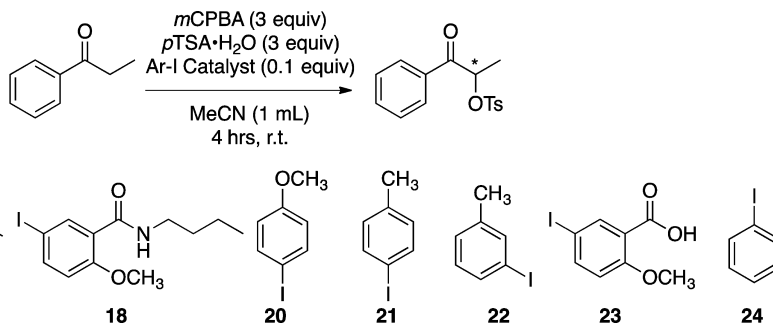
**Table 4. Oxidative  $\alpha$ -Oxytosylation of Propiophenone for 1 h at 50°C**

entry	catalyst	yield (%) <sup>a,b</sup>
1	9	63 ± 2
2	10	57 ± 2
3	15	43 ± 1
4	16	52 ± 3
5	17	63 ± 1
6	18	68 ± 1
7	19	48 ± 1

<sup>a</sup>Average yields of triplicate runs employing tetraglyme as the internal standard. <sup>b</sup>On 0.1 mmol scale.

These rate studies provided us with the necessary information to design a highly effective hypervalent iodine(III) catalyst while the installation of chiral information was still allowed via an amide bond in the context of our broader strategy to employ a peptide iodoarene catalyst scaffold for enantioselective processes. From our initial rate investigations, it is apparent that attaching the amide moiety to the iodoarene has some effect on the catalytic activity. One might presume that the presence of the electron-withdrawing amide on the arene would hinder the oxidation of the iodine(I)–arene catalyst to its active iodine(III) state. Alternatively, its presence on the iodoarene could also facilitate or hinder the displacement of the iodonium enolate intermediate in the second step of the reaction. In order to probe the specific influence of the amide moiety on the reactivity of the iodoarene benzamides, a series of structural analogs of our lead catalyst 18 was screened at room temperature for 4 h (Table 5, entries 3–7). Namely, 4-iodoanisole 20 and 4-iodotoluene 21 serve to probe the effects of the para-situated electron donor resident in lead catalyst 18 without the influence of the meta-oriented amide. Additionally,

3-iodotoluene 22 serves to probe the possible influence of replacing the electron-withdrawing amide group with an inductive donor (i.e., methyl) in the meta position relative to the iodine atom. Catalyst 23, 5-iodo-2-methoxybenzoic acid, positions the iodine and methoxy groups para to one another but contains a carboxylic acid functionality rather than an amide functionality meta to the iodine. Iodobenzene 24 evaluates the direct influence of incorporating an amide functionality on the activity of iodoarene catalysts as well as provides a benchmark for comparison of our benzamide catalysts to previous studies.<sup>34,41</sup> Of the analogs depicted in Table 5, catalysts 3-iodotoluene 22 and iodobenzene 24 were the most reactive, returning product in 53 and 52% yield, respectively (entries 5 and 7). Nevertheless, incorporation of the amide functionality (i.e., 18) in the meta position relative to I resulted in just a ~15% reduction in product yield, indicating that benzamide-modified aryl iodides are somewhat less reactive than the well-studied iodobenzene catalysts 22 and 24.<sup>34,41</sup> Somewhat surprisingly, catalyst 18 was a slightly more efficient catalyst than one of the most commonly employed catalyst for catalytic hypervalent iodine chemistry, 4-iodotoluene (21).<sup>34,35,41</sup> Similar trends were evident when comparing the *p*-iodobenzamide 10 with the comparatively more electron rich 4-iodoanisole 20 and 4-iodotoluene 21. Despite making significant changes to the electronics of the aryl iodide, catalysts 10 reacts only slightly slower than 20 and 21 (i.e., 19, 33, and 30% respectively at 4 h), particularly as compared to the much more sluggish *m*-substituted iodobenzamide 8 (i.e., 3% yield after 48 h, Table 1, entry 1). These data seem to suggest that electronic perturbations of the iodoarene have relatively little effect on the overall rate of the  $\alpha$ -oxytosylation reaction. Conversely, structural modifications that stabilize the I(III) state of the catalyst (see ortho-substituted benzamides 8 and 11–14) can dramatically retard the rate of reaction. Taken together, these data are consistent with a rate-determining step of the transformation that hinges on the attack of the I(III) catalyst by the enol tautomer of the substrate. More specifically, it seems that significant rate reductions for the  $\alpha$ -oxytosylation are only apparent when ortho-situated Lewis bases are available

**Table 5. Structural Analogues of Lead Catalyst 18**

entry	catalyst	yield (%) <sup>a,b</sup>
1	10	19 ± 3
2	18	44 ± 2
3	4-iodoanisole 20	33 ± 4
4	4-iodotoluene 21	30 ± 3
5	3-iodotoluene 22	53 ± 1
6	5-iodo-2-methoxybenzoic acid 23	40 ± 3
7	iodobenzene 24	52 ± 2

<sup>a</sup>Average yields of triplicate runs employing tetraglyme as the internal standard. <sup>b</sup>On 0.1 mmol scale.

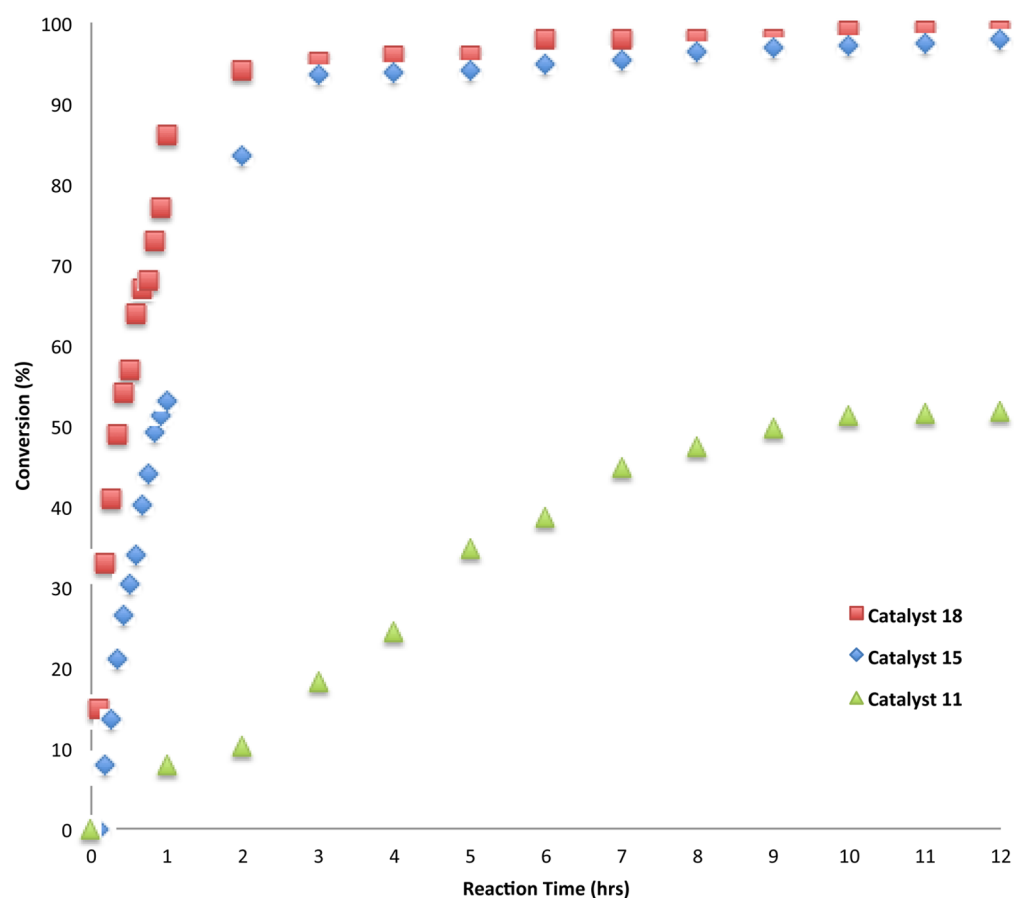


Figure 3.  $^1\text{H}$  NMR relative rate study of the oxidation of catalysts 18, 15, and 11 to their I(III) state.

to stabilize the I(III) state of the catalyst. Less significant rate changes are apparent when the iodoarene is modified with additional electron donors, but the effects on the rate of the transformation are comparatively much smaller than those observed upon incorporation of an ortho-disposed Lewis base. Finally, these data suggest that the presence of an amide linkage, which is critical for our peptide-based scaffold (see 6, Figure 1), does not appreciably affect the reactivity of the iodoarene site, provided that the amide is situated in the meta position relative the iodine atom, thus preventing coordinative interaction with the iodine active site of the catalyst.

To further investigate the influence of arene substituents of the catalysts, an NMR rate study was conducted in order to probe the relative rates of oxidation of the iodine(I) precatalysts to their active hypervalent iodine(III) species (Figure 3). Catalysts 18, 15, and 11 were chosen for this study because they represent the best, intermediate, and worst catalysts with respect to the observed yields of the  $\alpha$ -tosyloxy ketone product.

Upon analysis of the results it is clear that the oxidized iodine(III) state of catalysts 18 and 15 are more easily accessible compared to that of catalyst 11. On the basis of the NMR analysis, catalysts 18 and 15 each reach >90% conversion to their corresponding I(III) congener after just 3 h at room temperature, while catalyst 11 reaches just 50% conversion to its I(III) analog after 12 h (Figure 3). It is interesting to note that while catalysts 15 and 18 oxidize at similar rates, catalyst 18 is more reactive in the  $\alpha$ -oxtosylation of propiophenone (cf. Table 2, entries 3 and 6; Table 4, entries 3 and 6). This indicates that further rate enhancement of 18 is achieved not only while the iodine(III) species are accessed but also during

the attack of the substrate enol tautomer onto the I(III) species. Despite these events occurring before the likely rate-determining step in the process, it is apparent from this preliminary NMR rate study that the electronics of the iodoarene can significantly affect the rate of the I(I) to I(III) oxidation.

Ultimately, catalyst 18 emerged as the most effective iodobenzamide catalyst in our series. To briefly demonstrate the utility of catalyst 18, we conducted a small substrate scope evaluation (Table 6, entries 1–6). Propiophenones containing

Table 6. Oxidative  $\alpha$ -Oxytosylation of Propiophenone Derivatives

entry	R	product	<i>n</i>	time (h)	temp (°C)	yield (%) <sup>a,b</sup>
1	CH <sub>3</sub>	25	1	36	50	87
2	OCH <sub>3</sub>	26	1	40	50	72
3	F	27	1	24	50	94
4	Cl	28	1	24	50	75
5	Br	29	1	24	50	85
6	H	30	0	24	50	94
7	H	7	1	24	50	99
8	H	7	1	48	r.t.	94

<sup>a</sup>Isolated yields after silica gel column chromatography. <sup>b</sup>On 1 mmol scale.

fluoro, chloro, bromo, methyl, and methoxy substituents located in the para position on the phenyl ring and acetophenone were converted to the desired  $\alpha$ -substituted products in good to excellent isolated yields (1 mmol scale). Additionally, syntheses of the  $\alpha$ -oxytosylated propiophenone **7** were successfully performed, resulting in 99% and 94% isolated yields for reactions conducted at 50 °C and room temperature, respectively (Table 6, entries 7 and 8).

## CONCLUSION

In summary, several iodoarene benzamides were synthesized and assessed as catalysts in the  $\alpha$ -oxytosylation of propiophenone in order to probe the effects of the amide linkage on the reactivity of the iodoarene site in I(III)-mediated chemistry. The highest yields were obtained from precatalyst **18**, which places the catalytically active iodine atom meta to the amide and para to an electron-donating methoxy group. Studies with analog structures **20–24** revealed that the presence of a meta-oriented amide surprisingly does not appreciably affect the reactivity of the iodine active site. Additionally, we evaluated the time course of the oxidation of catalyst **18** and two others in the initial *m*CPBA-mediated oxidation to the requisite I(III) intermediate by means of  $^1\text{H}$  NMR analysis. Finally, we demonstrated the utility of lead catalyst **18** in the  $\alpha$ -oxytosylation of a series of substituted aryl ketones. In the context of our ultimate goal of developing highly active and enantioselective peptide-based iodoarene catalysts, we have demonstrated that a meta orientation between the iodine and the amide linkage is ideal in terms of catalyst reactivity. Further studies are currently being conducted focusing on the incorporation of analogs of precatalyst **18** and derivatives into small peptide sequences that can serve as a vehicle to render the  $\alpha$ -oxytosylation of ketones and other hypervalent-iodine-mediated reactions enantioselective.

## EXPERIMENTAL SECTION

**General Experimental Information.** All reagents were purchased from commercial suppliers and used without further purification. All isolated products were purified by flash column chromatography using silica gel SDS 60 C.C. 40–63  $\mu\text{m}$ . All known compounds and iodobenzoic acid starting materials had  $^1\text{H}$  NMR and  $^{13}\text{C}$  NMR spectra consistent with previous literature reports.  $^1\text{H}$  and  $^{13}\text{C}$  NMR spectra were collected at ambient temperature on a 500 or 300 MHz NMR spectrometer. Chemical shifts are reported in parts per million (ppm) and referenced to residual solvent peaks (i.e.,  $\delta$  7.28 ppm for  $^1\text{H}$  NMR, 77 ppm for  $^{13}\text{C}$  NMR) in  $\text{CDCl}_3$ . Data are presented as follows: chemical shift, integration, multiplicity (*s* = singlet, *d* = doublet, *t* = triplet, *q* = quartet, *br* = broad, *m* = multiplet), and coupling constants (*J*, in hertz). Infrared (IR) spectra, reported in  $\text{cm}^{-1}$ , were collected using a Fourier transform spectrophotometer. Bands are characterized as strong (*s*), medium (*m*), weak (*w*), and broad (*br*). Compounds **12–19** are newly synthesized compounds and thus were characterized via  $^1\text{H}$  and  $^{13}\text{C}$  NMR, IR, melting point, and HRMS-TOF (ESI). Gas chromatograph (GC) analyses were conducted using an autosampler and a flame ionization detector (FID). The GC was equipped with a 30 m  $\times$  0.32 mm  $\times$  0.25  $\mu\text{m}$  GC column with an HP-5 stationary phase.

**General Procedure for Preparation of the *N*-Butyl-iodobenzamides.** *N*-Butyl-iodobenzamide catalysts **8–19** were synthesized from their corresponding carboxylic acids via a conventional amidation reaction by the formation of the acid chloride and subsequent displacement by butyl amine.

A representative procedure for the synthesis of *N*-butyl-4-iodobenzamide **10**<sup>56</sup> is as follows: The substrate 4-iodobenzoic acid (0.2 g, 0.66 mmol, 1.0 equiv) and triethylamine (0.18 mL, 1.32 mmol, 2.0 equiv) were dissolved in anhydrous DCM (2 mL) and stirred for 5

min at room temperature under nitrogen in a flame-dried round-bottom flask. The solution was cooled to 0 °C. Thionyl chloride (0.053 mL, 0.726 mmol, 1.1 equiv) was slowly added (dropwise over 20 min), and the resulting solution was allowed to stir at 0 °C for 1 h. The resulting mixture was brought to room temperature and stirred for 30 min. This solution was concentrated under vacuum and then redissolved in anhydrous DCM (2 mL). To this solution was added (dropwise over 10 min) 1-butylamine (0.072 mL, 0.726 mmol, 1.1 equiv), anhydrous DCM (2 mL), and triethylamine (0.18 mL, 1.32 mmol, 2.0 equiv). The resulting solution was stirred overnight at room temperature under nitrogen. The crude mixture was concentrated by rotary evaporation, diluted in DCM, and washed with 1 M HCl, and the aqueous layers were extracted with DCM ( $\times 3$ ). The organic layers were washed with  $\text{H}_2\text{O}$  ( $\times 2$ ) and saturated brine ( $\times 1$ ) and dried over sodium sulfate. The resulting product was filtered and concentrated by rotary evaporation. The crude product was purified by column chromatography on silica gel (20:80 EtOAc:hexanes) to give **10** as an orange solid (0.2819 g, 93%), mp 121–122 °C. IR (neat): 3312 (*br*), 3075 (*w*), 2959 (*w*), 2929 (*w*), 2862 (*w*), 1632 (*s*), 1587 (*w*), 1543, 1468 (*w*), 1008 (*w*)  $\text{cm}^{-1}$ .  $^1\text{H}$  NMR (500 MHz,  $\text{CDCl}_3$ ):  $\delta$  0.97–0.99 (3H, *t*, *J* = 7.5 Hz), 1.39–1.47 (2H, *m*), 1.59–1.65 (2H, *m*), 3.44–3.48 (2H, *m*), 6.14 (1H, *s*, *br*), 7.50, 7.51 (2H, *d*, *J* = 8.5 Hz), 7.79, 7.81 (2H, *d*, *J* = 8.0 Hz) ppm.  $^{13}\text{C}$  NMR (500 MHz,  $\text{CDCl}_3$ ):  $\delta$  13.7, 20.1, 31.7, 39.9, 98.1, 128.5, 134.3, 137.8, 166.7 ppm. HRMS (ESI): *m/z* found 304.0200, calcd for  $\text{C}_{11}\text{H}_{15}\text{INO}$  (*M* + *H*)<sup>+</sup> 304.0198.

**General Procedure for  $\alpha$ -Oxytosylation of Propiophenone, **7**,<sup>45,57</sup>** The relative rates of the prepared *N*-butyl-iodobenzamide catalysts **8–19** were evaluated in the  $\alpha$ -oxytosylation of propiophenone using the following representative procedure with catalyst **8**. Propiophenone **5** (13.3  $\mu\text{L}$ , 0.1 mmol, 1.0 equiv), *p*-toluenesulfonic acid monohydrate (57.1 mg, 0.3 mmol, 3 equiv), *m*-chloroperoxybenzoic acid (51.8 mg, 0.3 mmol, 3 equiv), and *N*-butyl-iodobenzamide catalyst **8** (3.0 mg, 0.01 mmol, 0.1 equiv) were dissolved in acetonitrile (1 mL) and stirred for the appropriate time (72, 48, 24, 4, or 1 h) and temperature (room temperature or 50 °C). After the prescribed time, the reaction was quenched upon addition of dimethyl sulfide (3 equiv). This solution was concentrated by rotary evaporation, diluted in DCM, and washed with aqueous saturated sodium bicarbonate ( $\times 3$ ). The organic layers were dried over sodium sulfate, filtered, and concentrated by rotary evaporation. The resulting product and a 0.05 mmol aliquot of tetraglyme [as internal standard (ISTD)] were added to 1 mL volumetric flasks, and the final volume was taken to 1 mL with DCM. All trials were ran in triplicate and injected into the GC in order to evaluate percent yields and their standard deviations (see procedure details below).

**General Procedure for Preparation of GC Standard Curves.** Stock solutions (1 M) of the desired tosylated propiophenone **7** and ISTD (tetraglyme) were prepared in DCM. Varying amounts of desired product (0.005, 0.01, 0.02, 0.03, 0.04, 0.05, 0.06, 0.07, 0.08, 0.09, and 0.100 mmol) and a constant 0.05 mmol aliquot of ISTD were added to 1 mL volumetric flasks. The final volume was taken to 1 mL with DCM. These samples were injected into the GC, and the peak area ratio [(product area)/(ISTD area)] was calculated. This ratio was plotted versus the concentration of the desired product to yield a linear relationship ( $r^2$  values greater than 0.997), thus correlating GC chromatogram peak areas with product concentration. Reported yields and standard deviations were collected from averaged triplicate runs with tetraglyme (0.05 M) employed as the ISTD.

**General Procedure for Percent Yield Determination via GC Analysis.** GC analyses were carried out within the following parameters: inlet temperature, 250 °C; 20:1 split at 130 mL/min; column flow, 6.5 mL/min; constant pressure; carrier gas, helium; FID temperature, 300 °C; temperature program, 100 °C for 3 min, 20 °C/min ramp to 320 °C. Reactions were quenched with dimethyl sulfide (3 equiv) at prescribed times followed by GC analysis. Yields were calculated from a standard curve of the product in concentrations ranging from 0.005 to 0.1 M. Reported yields and standard deviations were collected from averaged triplicate runs with tetraglyme (0.05 M) employed as the ISTD.

**General Procedure for Scaleup and Isolated Yield Determination (i.e., Data for Table 6).** Utilizing our best catalyst **18**, scaled-up syntheses (1 mmol scales) of  $\alpha$ -oxotolylated propiophenone **7** and a brief substrate scope were conducted to give isolated yields for **7** as well as compounds **25–30**.

Representative procedure for the synthesis of 1-oxo-1-*p*-tolylpropan-2-yl 4-methylbenzenesulfonate **25**:<sup>51</sup> 4'-methylpropiophenone (149  $\mu$ L, 1.0 mmol, 1.0 equiv), *p*-toluenesulfonic acid monohydrate (571 mg, 3 mmol, 3 equiv), *m*-chloroperoxybenzoic acid (518 mg, 3 mmol, 3 equiv), and iodobenzamide catalyst **18** (33 mg, 0.1 mmol, 0.1 equiv) were dissolved in acetonitrile (10 mL) and stirred for 36 h at 50 °C. The reaction was immediately quenched with dimethyl sulfide (3 equiv). This solution was concentrated by rotary evaporation, diluted in DCM, and washed with aqueous saturated sodium bicarbonate ( $\times 3$ ). The organic layers were dried over sodium sulfate, filtered, and concentrated by rotary evaporation. The crude product was purified by column chromatography on silica gel (20:80 EtOAc:hexanes) to give **25** as a white solid (0.2783 g, 87%).  $R_f = 0.29$ .  $^1\text{H NMR}$  (300 MHz,  $\text{CDCl}_3$ ):  $\delta$  1.59, 1.61 (3H, d,  $J = 6.9$  Hz), 2.44 (6H, s, br), 5.79 (1H, q,  $J = 7.2$  Hz), 7.30–7.27 (4H, m), 7.82–7.63 (4H, m) ppm.  $^{13}\text{C NMR}$  (90 MHz,  $\text{CDCl}_3$ ):  $\delta$  18.8, 21.6, 21.7, 76.6, 128.0, 128.9, 129.5, 129.8, 131.1, 133.5, 144.9, 145.0, 194.3 ppm.

**General Procedure for NMR Kinetic Profiles (i.e., Figure 3).** The activity of catalysts **18**, **15**, and **11** was evaluated by monitoring oxidation rates of the catalysts from their iodine(I) state to their corresponding iodine(III) state. The kinetic profiles were generated by dissolving *m*-chloroperoxybenzoic acid (51.8 mg, 0.3 mmol, 3 equiv) and the respective iodobenzamide catalyst (0.01 mmol, 0.1 equiv) in  $\text{CD}_3\text{CN}$  (1 mL). Due to rapid oxidation of compounds **15** and **18**,  $^1\text{H NMR}$  spectra were recorded every 5 min for 1 h and then were recorded every hour after the first hour (recorded spectra up to 12 h). Compound **11** had a slower oxidation rate; thus,  $^1\text{H NMR}$  spectra were recorded every hour starting at 0 h (recorded spectra up to 12 h). The percent conversion of the I(I) catalyst to its corresponding I(III) was determined via changes in well-resolved NMR signal integration values as a function of time.

**Characterization Data for All Reported Compounds.** *N*-Butyl-2-iodobenzamide, **8**.<sup>58</sup> Brown solid (0.2839 g, 94%), mp 90–91 °C. IR (neat): 3287 (br), 3055 (w), 2953 (s), 2865 (m), 1649 (s), 1585 (m), 1539 (s), 1463 (m), 1015 (w)  $\text{cm}^{-1}$ .  $^1\text{H NMR}$  (500 MHz,  $\text{CDCl}_3$ ):  $\delta$  0.97–1.00 (3H, t,  $J = 7.0$  Hz), 1.40–1.47 (2H, m), 1.59–1.65 (2H, m), 3.45–3.49 (2H, m), 6.11 (1H, s, br), 7.18–7.21 (1H, t,  $J = 8.0$  Hz), 7.73–7.74 (1H, d,  $J = 8.0$  Hz), 7.84 (1H, q,  $J = 8.0$  Hz), 8.10–8.11 (1H, t,  $J = 1.5$  Hz) ppm.  $^{13}\text{C NMR}$  (125 MHz,  $\text{CDCl}_3$ ):  $\delta$  13.8, 20.2, 31.5, 39.9, 92.4, 128.2, 128.3, 131.0, 139.8, 142.5, 169.4 ppm. HRMS (ESI):  $m/z$  found 304.0204, calcd for  $\text{C}_{11}\text{H}_{15}\text{INO}$  ( $\text{M} + \text{H}$ )<sup>+</sup> 304.0198.

*N*-Butyl-3-iodobenzamide, **9**.<sup>59</sup> White solid (0.2776 g, 92%), mp 70–71 °C. IR (neat): 3280 (br), 3063 (m), 2958 (s), 2930 (s), 2870 (m), 1634 (s), 1592 (m), 1555 (s), 1467 (s), 1062 (w)  $\text{cm}^{-1}$ ;  $^1\text{H NMR}$  (500 MHz,  $\text{CDCl}_3$ ):  $\delta$  0.97–1.00 (3H, t,  $J = 7.5$  Hz), 1.40–1.47 (2H, m), 1.59–1.65 (2H, m), 3.45–3.49 (2H, m), 6.13 (1H, s, br), 7.17–7.20 (1H, t,  $J = 7.5$  Hz), 7.72, 7.74 (1H, d,  $J = 10.5$  Hz), 7.83, 7.85 (1H, d,  $J = 8.0$  Hz), 8.11 (1H, s) ppm.  $^{13}\text{C NMR}$  (125 MHz,  $\text{CDCl}_3$ ):  $\delta$  13.8, 20.2, 31.7, 40.0, 94.3, 126.1, 130.2, 135.9, 137.0, 140.2, 166.0 ppm. HRMS (ESI):  $m/z$  found 304.0201, calcd for  $\text{C}_{11}\text{H}_{15}\text{INO}$  ( $\text{M} + \text{H}$ )<sup>+</sup> 304.0198.

*N*-Butyl-2-iodo-4,5-dimethoxybenzamide, **11**.<sup>60</sup> Brown solid (0.5207 g, 88%), mp 104–106 °C; IR (neat): 3264 (br), 2957 (m), 2930 (m), 2869 (w), 1638 (s), 1593 (m), 1543 (m), 1501 (m), 1025 (w)  $\text{cm}^{-1}$ ;  $^1\text{H NMR}$  (500 MHz,  $\text{CDCl}_3$ ):  $\delta$  0.97–1.00 (3H, t,  $J = 7.0$  Hz), 1.43–1.51 (2H, m), 1.62–1.67 (2H, m), 3.45–3.49 (2H, m), 3.90 (6H, s, br), 5.87 (1H, s, br), 7.03 (1H, s), 7.22 (1H, s) ppm.  $^{13}\text{C NMR}$  (125 MHz,  $\text{CDCl}_3$ ):  $\delta$  13.8, 20.3, 31.4, 40.0, 56.1, 56.3, 80.8, 112.0, 122.0, 134.6, 149.2, 150.4, 168.9 ppm. HRMS (ESI):  $m/z$  found 364.0411, calcd for  $\text{C}_{13}\text{H}_{19}\text{INO}_3$  ( $\text{M} + \text{H}$ )<sup>+</sup> 364.0410.

*N*-Butyl-2-iodo-5-methoxybenzamide, **12**. Brown solid (0.2699 g, 90%), mp 80–81 °C. IR (neat): 3287 (br), 3069 (w), 2957 (m), 2932 (m), 2862 (w) 1642 (s), 1584 (m), 1542 (m), 1467 (m), 1009 (w)  $\text{cm}^{-1}$ .  $R_f = 0.12$  (20:80 EtOAc:hexanes).  $^1\text{H NMR}$  (500 MHz,

$\text{CDCl}_3$ ):  $\delta$  0.97–1.00 (3H, t,  $J = 7.0$  Hz), 1.43–1.50 (2H, m), 1.62–1.68 (2H, m), 3.45–3.49 (2H, m), 3.81 (3H, s), 5.82 (1H, s, br), 6.69–6.71 (1H, m), 6.98, 6.99 (1H, d,  $J = 3.0$  Hz), 7.70–7.71 (1H, d,  $J = 9.0$  Hz) ppm.  $^{13}\text{C NMR}$  (125 MHz,  $\text{CDCl}_3$ ):  $\delta$  13.7, 20.2, 31.4, 39.9, 55.6, 80.6, 114.2, 117.6, 140.4, 143.2, 159.7, 169.1 ppm. HRMS (ESI):  $m/z$  found 334.0310, calcd for  $\text{C}_{12}\text{H}_{17}\text{INO}_2$  ( $\text{M} + \text{H}$ )<sup>+</sup> 334.0304.

*N*-Butyl-2-iodo-5-methylbenzamide, **13**. White solid (0.2250 g, 93%), mp 106–107 °C. IR (neat): 3292 (br), 2957 (w), 2925 (w), 2864 (w) 1643 (s), 1541 (m), 1458 (w), 1012 (w)  $\text{cm}^{-1}$ .  $R_f = 0.44$  (20:80 EtOAc:hexanes).  $^1\text{H NMR}$  (500 MHz,  $\text{CDCl}_3$ ):  $\delta$  0.98–1.00 (3H, t,  $J = 7.5$  Hz), 1.43–1.51 (2H, m), 1.62–1.68 (2H, m), 2.33 (3H, s), 3.45–3.49 (2H, m), 5.76 (1H, s, br), 6.92–6.94 (1H, m), 7.23–7.24 (1H, d,  $J = 2.0$  Hz), 7.72–7.73 (1H, d,  $J = 8.0$  Hz) ppm.  $^{13}\text{C NMR}$  (125 MHz,  $\text{CDCl}_3$ ):  $\delta$  13.8, 20.2, 20.9, 31.5, 39.8, 88.2, 129.2, 132.0, 138.4, 139.6, 142.3, 169.5 ppm. HRMS (ESI):  $m/z$  found 318.0374, calcd for  $\text{C}_{12}\text{H}_{17}\text{INO}$  ( $\text{M} + \text{H}$ )<sup>+</sup> 318.0355.

*N*-Butyl-2-iodo-3-methylbenzamide, **14**. Yellow solid (0.2153 g, 89%), mp 68–69 °C. IR (neat): 3283 (br), 2957 (m), 2686 (w) 1640 (s), 1546 (m), 1476 (m), 1036 (w)  $\text{cm}^{-1}$ .  $R_f = 0.19$  (20:80 EtOAc:hexanes).  $^1\text{H NMR}$  (500 MHz,  $\text{CDCl}_3$ ):  $\delta$  0.97–1.00 (3H, t,  $J = 3.5$  Hz), 1.42–1.49 (2H, m), 1.61–1.67 (2H, m), 2.50 (3H, s), 3.45–3.49 (2H, m), 5.75 (1H, br), 7.10–7.13 (1H, m), 7.26–7.27 (2H, t,  $J = 2.0$  Hz) ppm.  $^{13}\text{C NMR}$  (125 MHz,  $\text{CDCl}_3$ ):  $\delta$  13.8, 20.2, 29.2, 31.4, 39.8, 99.3, 125.0, 128.1, 130.3, 142.8, 144.3, 170.4 ppm. HRMS (ESI):  $m/z$  found 318.0377, calcd for  $\text{C}_{12}\text{H}_{17}\text{INO}$  ( $\text{M} + \text{H}$ )<sup>+</sup> 318.0355.

*N*-Butyl-3-iodo-2-methylbenzamide, **15**. Light brown solid (0.2178 g, 90%), mp 98–99 °C. IR (neat): 3286 (br), 2955 (w), 2928 (w), 2862 (w), 1634 (s), 1581 (w), 1536 (m), 1433 (w), 999 (w)  $\text{cm}^{-1}$ .  $R_f = 0.28$  (20:80 EtOAc:hexanes).  $^1\text{H NMR}$  (500 MHz,  $\text{CDCl}_3$ ):  $\delta$  0.97–1.00 (3H, t,  $J = 7.5$  Hz), 1.40–1.47 (2H, m), 1.58–1.64 (2H, m), 2.52 (3H, s), 3.43–3.48 (2H, m), 5.75 (1H, s, br), 6.90–6.93 (1H, t,  $J = 7.5$  Hz), 7.30 (1H, d,  $J = 0.50$  Hz), 7.88–7.90 (1H, m) ppm.  $^{13}\text{C NMR}$  (125 MHz,  $\text{CDCl}_3$ ):  $\delta$  13.8, 20.1, 25.6, 31.6, 39.7, 103.4, 126.5, 127.3, 138.2, 138.4, 140.5, 169.6 ppm. HRMS (ESI):  $m/z$  found 318.0377, calcd for  $\text{C}_{12}\text{H}_{17}\text{INO}$  ( $\text{M} + \text{H}$ )<sup>+</sup> 318.0355.

*N*-Butyl-3-iodo-4-methylbenzamide, **16**. Brown oil (0.0871 g, 72%). IR (neat): 3300 (br), 2957 (m), 2929 (m), 2870 (w), 1636 (s), 1600 (w), 1547 (s), 1481 (m), 1032 (w)  $\text{cm}^{-1}$ .  $R_f = 0.33$  (20:80 EtOAc:hexanes).  $^1\text{H NMR}$  (500 MHz,  $\text{CDCl}_3$ ):  $\delta$  0.97–1.00 (3H, t,  $J = 7.5$  Hz), 1.40–1.47 (2H, m), 1.59–1.65 (2H, m), 2.48 (3H, s), 3.44–3.48 (2H, m), 6.10 (1H, s, br), 7.30 (1H, s), 7.65–7.66 (1H, m), 8.20 (1H, d,  $J = 2.0$  Hz) ppm.  $^{13}\text{C NMR}$  (125 MHz,  $\text{CDCl}_3$ ):  $\delta$  13.8, 20.2, 28.1, 31.7, 39.9, 100.9, 126.7, 129.6, 134.0, 137.4, 145.0, 165.8 ppm. HRMS (ESI):  $m/z$  found 318.0377, calcd for  $\text{C}_{12}\text{H}_{17}\text{INO}$  ( $\text{M} + \text{H}$ )<sup>+</sup> 318.0355.

*N*-Butyl-3-iodo-4-methoxybenzamide, **17**. Brown solid (0.4105 g, 69%), mp 71–72 °C. IR (neat): 3315 (br), 2958 (m), 2932 (m), 2870 (w), 1631 (s), 1595 (s), 1548 (s), 1487 (s), 1016 (w)  $\text{cm}^{-1}$ .  $R_f = 0.32$  (20:80 EtOAc:hexanes).  $^1\text{H NMR}$  (500 MHz,  $\text{CDCl}_3$ ):  $\delta$  0.95–0.99 (3H, t,  $J = 7.5$  Hz), 1.38–1.45 (2H, m), 1.58–1.64 (2H, m), 3.42–3.46 (2H, m), 3.93 (3H, s), 6.20 (1H, s, br), 6.82–6.84 (1H, d,  $J = 0.50$  Hz), 7.78–7.80 (1H, m), 8.17–8.18 (1H, d,  $J = 2.5$  Hz) ppm.  $^{13}\text{C NMR}$  (125 MHz,  $\text{CDCl}_3$ ):  $\delta$  13.8, 20.2, 31.8, 39.9, 56.6, 85.6, 110.2, 128.9, 129.0, 138.1, 160.4, 165.7 ppm. HRMS (ESI):  $m/z$  found 334.0333, calcd for  $\text{C}_{12}\text{H}_{17}\text{INO}_2$  ( $\text{M} + \text{H}$ )<sup>+</sup> 334.0304.

*N*-Butyl-5-iodo-2-methoxybenzamide, **18**. White solid (0.2240 g, 75%), mp 41–42 °C. IR (neat): 3405 (br), 2957 (m), 2930 (m), 2870 (w), 1643 (s), 1586 (m), 1534 (s), 1477 (s), 1019 (m)  $\text{cm}^{-1}$ .  $R_f = 0.31$  (20:80 EtOAc:hexanes).  $^1\text{H NMR}$  (500 MHz,  $\text{CDCl}_3$ ):  $\delta$  0.94–0.97 (3H, t,  $J = 7.0$  Hz), 1.37–1.44 (2H, m), 1.56–1.62 (2H, m), 3.42–3.46 (2H, m), 3.94 (3H, s), 6.72, 6.74 (1H, d,  $J = 9.0$  Hz), 7.66–7.69 (1H, m), 7.75 (1H, s, br), 8.45–8.46 (1H, d,  $J = 2.0$  Hz) ppm.  $^{13}\text{C NMR}$  (125 MHz,  $\text{CDCl}_3$ ):  $\delta$  13.8, 17.6, 20.2, 31.6, 39.6, 56.2, 83.7, 113.7, 123.9, 140.7, 157.2, 163.7 ppm. HRMS (ESI):  $m/z$  found 334.0333, calcd for  $\text{C}_{12}\text{H}_{17}\text{INO}_2$  ( $\text{M} + \text{H}$ )<sup>+</sup> 334.0304.

*N*-Butyl-5-iodo-2-methoxy-4-methylbenzamide, **19**. Brown solid (0.1164 g, 98%), mp 117–118 °C. IR (neat): 3401 (br), 2955 (m), 2935 (m), 2859 (w), 1646 (s), 1593 (m), 1530 (s), 1460 (m), 1033 (w)  $\text{cm}^{-1}$ .  $R_f = 0.22$  (20:80 EtOAc:hexanes).  $^1\text{H NMR}$  (500 MHz,



CDCl<sub>3</sub>):  $\delta$  0.97–0.99 (3H, t,  $J$  = 7.0 Hz), 1.39–1.47 (2H, m), 1.58–1.64 (2H, m), 2.47 (3H, s), 3.45–3.49 (2H, m), 3.96 (3H, s), 6.86 (1H, s), 7.76 (1H, s, br), 8.58 (1H, s) ppm. <sup>13</sup>C NMR (125 MHz, CDCl<sub>3</sub>):  $\delta$  13.8, 20.3, 28.4, 31.6, 39.5, 56.1, 90.6, 113.0, 121.1, 142.0, 146.1, 157.3, 163.7 ppm. HRMS (ESI):  $m/z$  found 348.0491, calcd for C<sub>13</sub>H<sub>19</sub>INO<sub>2</sub> (M + H)<sup>+</sup> 348.0460.

**1-(4-Methoxyphenyl)-1-oxopropan-2-yl 4-Methylbenzenesulfonate, 26.**<sup>45</sup> White solid (0.2408 g, 72%).  $R_f$  = 0.183 (20:80 EtOAc:hexanes). <sup>1</sup>H NMR (300 MHz, CDCl<sub>3</sub>):  $\delta$  1.59, 1.61 (3H, d,  $J$  = 6.9 Hz) 2.43 (3H, s), 3.89 (3H, s), 5.76 (1H, q,  $J$  = 6.9), 7.27–7.30 (2H, m), 7.76, 7.79 (2H, d,  $J$  = 8.4), 7.88–7.93 (2H, m) 7.89–7.91 ppm (2H, m) ppm. <sup>13</sup>C NMR (90 MHz, CDCl<sub>3</sub>):  $\delta$  18.9, 21.7, 55.6, 76.8, 114.0, 126.5, 128.0, 129.7, 131.2, 133.5, 145.0, 164.1, 193.1 ppm.

**1-(4-Fluorophenyl)-1-oxopropan-2-yl 4-Methylbenzenesulfonate, 27.**<sup>57</sup> White solid (0.3030 g, 94%).  $R_f$  = 0.33 (20:80 EtOAc:hexanes). <sup>1</sup>H NMR (500 MHz, CDCl<sub>3</sub>):  $\delta$  1.60, 1.61 (3H, d,  $J$  = 7.0 Hz), 2.44 (3H, s), 5.72 (1H, q,  $J$  = 7.0 Hz), 7.14–7.17 (2H, t,  $J$  = 8.0 Hz), 7.29–7.31 (2H, m), 7.76–7.78 (2H, m), 7.95–7.98 (2H, m) ppm. <sup>13</sup>C NMR (125 MHz, CDCl<sub>3</sub>):  $\delta$  18.6, 21.7, 76.8, 115.9, 116.1, 128.0, 129.8, 131.6, 131.7, 133.4, 145.2, 165.1, 167.1, 193.4 ppm.

**1-(4-Chlorophenyl)-1-oxopropan-2-yl 4-Methylbenzenesulfonate, 28.**<sup>57</sup> White solid (0.2464 g, 75%).  $R_f$  = 0.32 (20:80 EtOAc:hexanes). <sup>1</sup>H NMR (500 MHz, CDCl<sub>3</sub>):  $\delta$  1.60, 1.61 (3H, d,  $J$  = 7.0 Hz), 2.45 (3H, s), 5.71 (1H, q,  $J$  = 7.0 Hz), 7.30, 7.31 (2H, d,  $J$  = 8.0 Hz), 7.44, 7.46 (2H, d,  $J$  = 8.5 Hz), 7.75, 7.77 (2H, d,  $J$  = 8.5 Hz), 7.85, 7.87 (2H, d,  $J$  = 9.0 Hz) ppm. <sup>13</sup>C NMR (125 MHz, CDCl<sub>3</sub>):  $\delta$  18.6, 21.7, 76.8, 128.0, 129.1, 129.8, 130.3, 132.0, 133.3, 140.4, 145.2, 194.0 ppm.

**1-(4-Bromophenyl)-1-oxopropan-2-yl 4-Methylbenzenesulfonate, 29.**<sup>57</sup> White solid (0.3266 g, 85%).  $R_f$  = 0.37 (20:80 EtOAc:hexanes). <sup>1</sup>H NMR (300 MHz, CDCl<sub>3</sub>):  $\delta$  1.59, 1.61 (3H, d,  $J$  = 6.9 Hz), 2.44 (3H, s), 5.69 (1H, q,  $J$  = 6.9 Hz), 7.31 (2H, s), 7.59–7.63 (2H, m), 7.74–7.80 (4H, m) ppm. <sup>13</sup>C NMR (90 MHz, CDCl<sub>3</sub>):  $\delta$  18.6, 21.7, 76.8, 127.9, 129.2, 129.9, 130.3, 132.1, 132.4, 133.3, 145.2, 194.1 ppm.

**$\alpha$ -Tosyloxyacetophenone, 30.**<sup>57</sup> White solid (0.2729 g, 94%).  $R_f$  = 0.24 (20:80 EtOAc:hexanes). <sup>1</sup>H NMR (500 MHz, CDCl<sub>3</sub>):  $\delta$  2.47 (3H, s), 5.29 (2H, s), 7.36, 7.38 (2H, d,  $J$  = 8.0 Hz), 7.48–7.51 (2H, m), 7.61–7.64 (1H, m), 7.85–7.88 (4H, m) ppm. <sup>13</sup>C NMR (125 MHz, CDCl<sub>3</sub>):  $\delta$  21.7, 70.0, 128.0, 128.2, 128.9, 129.9, 132.7, 133.8, 134.2, 145.3, 190.3 ppm.

## ■ ASSOCIATED CONTENT

### 📄 Supporting Information

The Supporting Information is available free of charge on the ACS Publications website at DOI: 10.1021/acs.joc.5b02129.

The standard curve for GC yield determination as well as copies of <sup>1</sup>H and <sup>13</sup>C NMR spectra of all synthesized compounds (PDF)

## ■ AUTHOR INFORMATION

### Corresponding Author

\*E-mail: dwhiteh@clemsun.edu

### Notes

The authors declare no competing financial interest.

## ■ ACKNOWLEDGMENTS

We gratefully acknowledge Clemson University and the CU Department of Chemistry for financial support. We also thank Ms. Nastaran Salehi for assistance with HRMS analysis.

## ■ REFERENCES

- (1) Moriarty, R. M. *J. Org. Chem.* **2005**, *70*, 2893.
- (2) Berthiol, F. *Synthesis* **2015**, *47*, 587–603.
- (3) *Hypervalent Iodine Chemistry—Modern Developments in Organic Synthesis*; Wirth, T., Ed.; Springer: Berlin, 2003; Vol. 224.

- (4) Zhdankin, V. V.; Stang, P. *Chem. Rev.* **2002**, *102*, 2523.
- (5) Moriarty, R. M.; Prakash, O. *Org. React.* **2001**, *57*, 327.
- (6) Wirth, T.; Hirt, U. H. *Synthesis* **1999**, *1999*, 1271–1287.
- (7) Silva, L. F., Jr.; Olofsson, B. *Nat. Prod. Rep.* **2011**, *28*, 1722–1754.
- (8) Zhdankin, V. V.; Stang, P. J. *Chem. Rev.* **2008**, *108*, 5299.
- (9) Uyanik, M.; Ishihara, K. *Chem. Commun.* **2009**, 2086–2099.
- (10) Satam, V.; Harad, A.; Rajule, R.; Pati, H. *Tetrahedron* **2010**, *66*, 7659–7706.
- (11) Moriarty, R. M.; Prakash, O. *Org. React.* **1999**, *54*, 273.
- (12) Wirth, T.; Hirt, U. H. *Tetrahedron: Asymmetry* **1997**, *8*, 23–26.
- (13) Hirt, U. H.; Spingler, B.; Wirth, T. *J. Org. Chem.* **1998**, *63*, 7674–7679.
- (14) Kopusov, A. Y.; Boyarskikh, V. V.; Zhdankin, V. V. *Org. Lett.* **2004**, *6*, 3613–3615.
- (15) Pouységu, L.; Deffieux, D.; Quideau, S. *Tetrahedron* **2010**, *66*, 2235.
- (16) Ciufolini, M. A.; Braun, N. A.; Canesi, S.; Ousmer, M.; Chang, J.; Chai, D. *Synthesis* **2007**, *2007*, 3759.
- (17) Magdziak, D.; Meek, S. J.; Pettus, T. R. R. *Chem. Rev.* **2004**, *104*, 1383.
- (18) Allen, A. E.; MacMillan, D. W. C. *J. Am. Chem. Soc.* **2011**, *133*, 4260.
- (19) Dong, D.-Q.; Hao, S.-H.; Wang, Z.-L.; Chen, C. *Org. Biomol. Chem.* **2014**, *12*, 4278–4289.
- (20) Uyanik, M.; Suzuki, D.; Yasui, T.; Ishihara, K. *Angew. Chem., Int. Ed.* **2011**, *50*, 5331–5334.
- (21) Uyanik, M.; Yasui, T.; Ishihara, K. *Bioorg. Med. Chem. Lett.* **2009**, *19*, 3848.
- (22) Moriarty, R. M.; Vaid, R. K.; Hopkins, T. E.; Vaid, B. K.; Prakash, O. *Tetrahedron Lett.* **1990**, *31*, 201.
- (23) Hong, K. B.; Johnston, J. N. *Org. Lett.* **2014**, *16*, 3804–3807.
- (24) Chen, H.; Kaga, A.; Chiba, S. *Org. Lett.* **2014**, *16*, 6136–6139.
- (25) Martínez, C.; Muñiz, K. *Angew. Chem., Int. Ed.* **2015**, *54*, 8287–8291.
- (26) Pohnert, G. *J. Prakt. Chem.* **2000**, *342*, 731–734.
- (27) Jiang, Q.; Zhao, A.; Xu, B.; Jia, J.; Liu, X.; Guo, C. *J. Org. Chem.* **2014**, *79*, 2709–2715.
- (28) Moriarty, R. M.; Vaid, R. K.; Koser, G. F. *Synlett* **1990**, *1990*, 365–383.
- (29) Berkessel, A.; Groger, H.; MacMillan, D. *Asymmetric Organocatalysis*; Wiley-VCH: Weinheim, Germany, 2005.
- (30) MacMillan, D. W. C. *Nature* **2008**, *455*, 304–308.
- (31) Barbas, C. F., III. *Angew. Chem., Int. Ed.* **2008**, *47*, 42–47.
- (32) Dohi, T.; Kita, Y. *Chem. Commun.* **2009**, 2073–2085.
- (33) Ochiai, M.; Miyamoto, K. *Eur. J. Org. Chem.* **2008**, *2008*, 4229.
- (34) Ochiai, M.; Takeuchi, Y.; Katayama, T.; Sueda, T.; Miyamoto, K. *J. Am. Chem. Soc.* **2005**, *127*, 12244.
- (35) Dohi, T.; Maruyama, A.; Yoshimura, M.; Morimoto, K.; Tohma, H.; Kita, Y. *Angew. Chem., Int. Ed.* **2005**, *44*, 6193.
- (36) Dohi, T.; Kita, Y. *Kagaku* **2006**, *61*, 68–69.
- (37) Stang, P. J.; Zhdankin, V. V. *Chem. Rev.* **1996**, *96*, 1123–1178.
- (38) Koser, G. F.; Relenyi, A. G.; Kalos, A. N.; Rebrovic, L.; Wettach, R. H. *J. Org. Chem.* **1982**, *47*, 2487.
- (39) Moriarty, R. M.; Penmasta, R.; Awasthi, A. K.; Epa, W. R.; Prakash, I. *J. Org. Chem.* **1989**, *54*, 1101.
- (40) Nabana, T.; Togo, H. *J. Org. Chem.* **2002**, *67*, 4362.
- (41) Yamamoto, Y.; Togo, H. *Synlett* **2006**, 798–800.
- (42) Yamamoto, Y.; Kawano, Y.; Toy, P. H.; Togo, H. *Tetrahedron* **2007**, *63*, 4680–4687.
- (43) Richardson, R. D.; Zayed, J. M.; Altermann, S.; Smith, D.; Wirth, T. *Angew. Chem., Int. Ed.* **2007**, *46*, 6529.
- (44) Zhang, B.; Han, L.; Hu, J.; Yan, J. *Tetrahedron Lett.* **2014**, *55*, 5851–5854.
- (45) Basdevant, B.; Legault, C. Y. *J. Org. Chem.* **2015**, *80*, 6897–6902.
- (46) Parra, A.; Reboredo, S. *Chem. - Eur. J.* **2013**, *19*, 17244–17260.
- (47) Brown, M.; Farid, U.; Wirth, T. *Synlett* **2013**, *24*, 424–431.
- (48) Hirt, U. H.; Schuster, M. F. H.; French, A. N.; Wiest, O. G.; Wirth, T. *Eur. J. Org. Chem.* **2001**, *2001*, 1569–1579.

- (49) Yu, J.; Cui, J.; Hou, X.-S.; Liu, S.-S.; Gao, W.-C.; Jiang, S.; Tian, J.; Zhang, C. *Tetrahedron: Asymmetry* **2011**, *22*, 2039–2055.
- (50) Guilbault, A.-A.; Legault, C. Y. *ACS Catal.* **2012**, *2*, 219–222.
- (51) Guilbault, A. – A.; Basdevant, B.; Wanie, V.; Legault, C. Y. *J. Org. Chem.* **2012**, *77*, 11283–11295.
- (52) Basdevant, B.; Legault, C. Y. *Org. Lett.* **2015**, *17*, 4918–4921.
- (53) Jarvo, E. R.; Miller, S. J. *Tetrahedron* **2002**, *58*, 2481–2495.
- (54) Miller, S. J. *Acc. Chem. Res.* **2004**, *37*, 601–610.
- (55) Su, J. T.; Goddard, W. A., III *J. Am. Chem. Soc.* **2005**, *127*, 14146–14147.
- (56) Wang, T.; Yuan, L.; Zhao, Z.; Shao, A.; Gao, M.; Huang, Y.; Xiong, F.; Zhang, H.; Zhao, J. *Green Chem.* **2015**, *17*, 2741–2744.
- (57) John, O. R. S.; Killeen, N. M.; Knowles, D. A.; Yau, S. C.; Bagley, M. C.; Tomkinson, N. C. O. *Org. Lett.* **2007**, *9*, 4009–4012.
- (58) Schröder, N.; Wencel-Delord, J.; Glorius, F. *J. Am. Chem. Soc.* **2012**, *134*, 8298.
- (59) Wang, L.; Zhong, C.; Xue, P.; Fu, E. *J. Org. Chem.* **2011**, *76*, 4874–4883.
- (60) Madich, Y.; Denis, J. D.; Ortega, A.; Martínez, C.; Matrane, A.; Belachemi, L.; de Lera, Á. R.; Alvarez, R.; Aurrecoechea, J. M. *Synthesis* **2013**, *45*, 2009–2017.